Stability Analysis of Quadruped Bounding with Asymmetrical Body Mass Distribution

Hong Zou
Department of Mechanical and Industrial Engineering
The University of Iowa
Iowa City, IA USA
hong-zou@uiowa.edu

James P. Schmiedeler
Department of Mechanical Engineering
The Ohio State University
Columbus, OH USA
schmiedeler.2@osu.edu

***Abstract*—An analytical stability criterion for bounding of quadrupeds with asymmetrical mass distribution is developed in this work. Bounding is found to be passively stable when the dimensionless pitch moment of inertia of the body is less than $1-\beta^2$, where β is a dimensionless measure of the asymmetry. The criterion is derived under the assumptions of infinite leg stiffness and no energy loss. Simulation results show that the criterion is independent of the value of leg stiffness and a conservative estimate of the critical inertia value when energy losses are modeled with linear damping. Body symmetry appears to be more favorable to stable bounding than asymmetry, but only slightly so in practicality.**

Keywords-legged locomotion; quadruped; bounding; stability

I. Introduction

The success of Raibert's [14] locomotion control algorithms in generating dynamically stable gaits for his monopod, biped, and quadruped robots has inspired the development of a number of subsequent analytical models that provide further theoretical understanding of the experimental results. Koditschek and Bühler [8] investigated the vertical dynamics of a model of Raibert's monopod with nonlinear and linear spring laws using different parametric simplifications. They presented a stability analysis using discrete dynamical system theory and demonstrated that the existence of period-2 behavior was very similar to the experimentally observed "limping gait". Vakakis et al. [18] developed a more complete model of the system by relaxing the assumption that thrust was exerted instantaneously. They constructed the global bifurcation diagram, showing that the period-doubling cascade leads to chaos and that an appropriately selected duration of thrust can ensure stable period-1 behavior. M'Closkey and Burdick [11] further extended this to a two degree-of-freedom model that included both forward and vertical hopping dynamics. Their global bifurcation diagrams developed for both approximate and exact return maps showed that the period-doubling behavior is preserved under lateral motion. They also derived an analytical estimate of stance time to be used in the foot placement algorithm. Li and He [9] argued that the nonlinearity and discontinuity of the locomotion dynamics severely limit the usefulness of the discrete dynamical system theory. They combined perturbation and energy balance methods to study the dynamics and stability of hopping in both a nonlinear and linear spring model.

Raibert's quadruped was capable of trotting, pacing, and bounding [15], but the majority of quadruped analysis has focused on pitch stability in bounding. Murphy [16] developed a model of a planar quadruped with one massive front leg and one massive rear leg to study control of vertical motion, forward velocity, and body attitude. In simulation, he found that the model maintained a stable bounding gait without active attitude control when a dimensionless moment of inertia was less than unity. Neishtadt and Li [12] proposed an analytical proof of this stability criterion using a simplified model that neglected forward motion and assumed a small pitch angle. With fixed levels of damping in the legs or across the hip joints, asymptotical stability with respect to change in energy was obtained. Berkemeier [1] analyzed a similar model, formulating approximate return maps for both bounding and pronking, the latter being an approximation of trotting or pacing in the planar case. Berkemeier's results also indicate that bounding is passively stable in pitch when the dimensionless body inertia is less than unity. In pronking, however, he found the stability to exhibit a coupling between height and inertia.

In all of these quadruped models, the body mass is symmetrically distributed such that the center of mass coincides with the geometric center of the body. Indeed, this matches the design of Raibert's quadruped [15], and body mass symmetry has characterized other bounding quadruped robots built to date: Scamper2 [4], SCOUT II [13], Patrush-I [6], and Tekken-I [7]. In contrast, most quadruped animals have an asymmetrical mass distribution with the mass center located closer to the shoulder joints than to the hip joints [2] [10]. As a result, the front legs tend to provide more vertical thrust, while the rear legs provide more longitudinal thrust [3] [5]. Schmiedeler and Waldron [17] investigated these and other effects of body asymmetry in their impulsive model of quadruped galloping, but they did not analyze stability.

This paper develops a general bounding stability criterion that is applicable to quadrupeds with asymmetrical body mass distribution. The objectives of the work are to assess the impact of asymmetry on stability and to provide an analytical

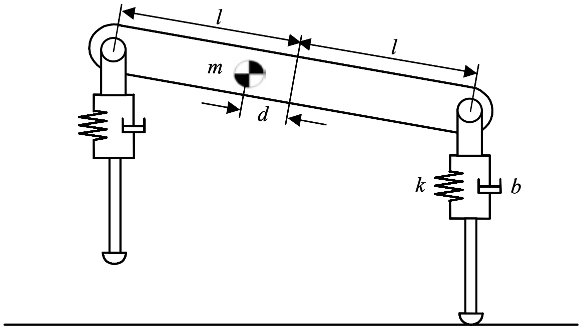

Figure 1. Schematic of bounding model.

tool to aid in the design of quadruped robots. An asymmetrical mass distribution offers some potential advantages such as exploiting the specialized functions of the front and rear legs. The remainder of the paper is organized as follows. Section II describes the bounding model, and the equations of motion and stability criterion are developed in Section III. Section IV presents simulation results that validate the criterion, and conclusions are presented in Section V.

II. Model Description

The planar quadruped model, shown in Fig. 1, is identical to Berkemeier's [1] with the exception of the asymmetrical mass distribution, represented by the parameter *d,* the distance between the mass center and the geometric center of the body. In the figure, m is the body mass, l is one half the length between the shoulder and hip joints, *k* is the stiffness of the leg spring, and *b* is the coefficient of the linear damper in the leg. The legs are assumed to be massless. In bounding, the legs operate in front and rear pairs, so the two front legs are modeled with a single leg, as are the two rear legs. Thrust is provided by instantaneously changing the free length of the leg spring when the leg is maximally compressed. The model includes only pitch angular motion and vertical translation of the body, so forward motion is neglected. The heights of the rear and front legs can be expressed,

$$z_f = z - (l-d)\theta, \quad z_r = z + (l+d)\theta,$$

where z is the height of the mass center and θ is the pitch angle of the body, which is assumed to be small and measured positive in a counterclockwise sense. The subscripts "f" and "r" indicate quantities associated with the front and rear legs, respectively.

III. Stability Analysis

The formulation in this section follows closely the work of Neischtadt and Li [12], the most significant departure being the consideration of the entire bounding cycle rather than simply one half of it. For a symmetric body, the full cycle can be divided into two symmetric halves, one in which the front leg contacts the ground, and one in which the rear leg contacts the ground. Stability analysis of either half, therefore, directly addresses stability of the entire cycle. With an asymmetric body, however, the two portions of the cycle are no longer symmetric, so analysis of only one portion does not provide information about the entire cycle. In this work, the two portions of the cycle are referred two as the "rear half cycle" and the "front half cycle" despite the fact that their durations do not in general represent exact halves of the cycle.

To make the calculations in this section tractable, the damping and thrust in the legs are assumed to be negligible, as is common to the work of Neishtadt and Li [12] and Berkemeier [1]; therefore, there is no energy loss during the motion. These assumptions are relaxed in the simulation results presented in Section III to validate the stability criterion derived below.

A. Normalization of Hamiltonian System

With the coordinates chosen appropriately, the Hamiltonian of this system is equivalent to the total energy. The Hamiltonian during the flight phase is given by,

$$H_0 = \frac{1}{2}m\dot{z}^2 + \frac{1}{2}I\dot{\theta}^2 + mgz \,, \tag{1}$$

where g is the acceleration of gravity and the "*dot*" notation indicates derivatives with respect to time t. The Hamiltonian does not explicitly depend on time, and its value is invariant, so a conservative Hamiltonian system is obtained.

1) Rear-Normalization

The Hamiltonian of the system when the rear leg contacts the ground is given by,

$$H_r = H_0 + \frac{k_r}{2}\left(z_r - z_l\right)^2 , \tag{2}$$

where k_r is the stiffness of the rear leg and z_l is the height of the hip joint when the leg is at its free length. Normalized variables are introduced in order to simplify the analysis,

$$\hat{z} = \frac{z - z_l}{l+d}\,,\ \hat{I}_r = \frac{I}{m\left(l+d\right)^2}\,,\ \hat{k}_r = \frac{k_r}{m}\,,\ \hat{g}_r = \frac{g}{l+d}\,,\ \hat{\theta} = \theta\,. \tag{3}$$

This procedure is referred to as "*rear-normalization*" since it only applies to the rear half cycle. Note that it differs from the normalization of Neishtadt and Li [12]. After normalization, the height of the rear leg becomes,

$$\hat{z}_r = \hat{z} + \hat{\theta}\,. \tag{4}$$

Dividing both sides of (2) by $m(l+d)^2$ gives,

$$\hat{H}_r = \frac{1}{2}\dot{\hat{z}}^2 + \frac{1}{2}\hat{I}_r\dot{\hat{\theta}}^2 + \hat{g}_r\hat{z} + \frac{\hat{k}_r}{2}\left(\hat{z}+\hat{\theta}\right)^2 . \tag{5}$$

The corresponding conjugate momenta of $\hat{z}$ and $\hat{\theta}$ are,

$$p_{\hat{z}} = \frac{\partial \hat{H}_r}{\partial \dot{\hat{z}}} = \dot{\hat{z}}, \quad p_{\hat{\theta}} = \frac{\partial \hat{H}_r}{\partial \dot{\hat{\theta}}} = \hat{I}_r\dot{\hat{\theta}}\,.$$

Rewriting (5) in terms of the conjugate momenta yields,

$$\hat{H}_r = \frac{1}{2}{p_{\hat{z}}}^2 + \frac{1}{2}\frac{1}{\hat{I}_r}{p_{\hat{\theta}}}^2 + \hat{g}_r\hat{z} + \frac{\hat{k}_r}{2}\left(\hat{z}+\hat{\theta}\right)^2 .$$

In the rear half cycle, the equations of motion are given by,

$$\begin{aligned} &\dot{\hat{\theta}} = \frac{\partial \hat{H}_r}{\partial p_{\hat{\theta}}}, \quad \dot{\hat{z}} = \frac{\partial \hat{H}_r}{\partial p_{\hat{z}}}, \quad \dot{p}_{\hat{\theta}} = -\frac{\partial \hat{H}_r}{\partial \hat{\theta}} = \hat{k}_r\left(\hat{z}+\hat{\theta}\right), \\ &\dot{p}_{\hat{z}} = -\frac{\partial \hat{H}_r}{\partial \hat{z}} = -\hat{k}_r\left(\hat{z}+\hat{\theta}\right) - \hat{g}_r\,. \end{aligned} \tag{6}$$

2) Front-Normalization

When the front leg contacts the ground in the front half cycle, the Hamiltonian is,

$$H_f = H_0 + \frac{k_f}{2}\left(z_f - z_l\right)^2, \tag{7}$$

where k_f is the stiffness of the front leg. Here, a "*front-normalization*" of variables that is only applicable in the front half cycle is performed.

$$\hat{z} = \frac{z - z_l}{l-d},\ \hat{I}_f = \frac{I}{m\left(l-d\right)^2},\ \hat{k}_f = \frac{k_f}{m},\ \hat{g}_f = \frac{g}{l-d},\ \hat{\theta} = \theta. \tag{8}$$

The height of the front leg becomes,

$$\hat{z}_f = \hat{z} - \hat{\theta}. \tag{9}$$

Dividing the Hamiltonian in (7) by $m(l-d)^2$ yields,

$$\hat{H}_f = \frac{1}{2}\hat{\dot{z}}^2 + \frac{1}{2}\hat{I}_f\hat{\dot{\theta}}^2 + \hat{g}_f\hat{z} + \frac{\hat{k}_f}{2}\left(\hat{z} - \hat{\theta}\right)^2. \tag{10}$$

The conjugate momenta of $\hat{z}$ and $\hat{\theta}$ in the front half cycle are,

$$p_{\hat{z}} = \frac{\partial \hat{H}_f}{\partial \hat{\dot{z}}} = \hat{\dot{z}},\quad p_{\hat{\theta}} = \frac{\partial \hat{H}_f}{\partial \hat{\dot{\theta}}} = \hat{I}_f\hat{\dot{\theta}}.$$

Rewriting (10) in terms of conjugate momenta gives,

$$\hat{H}_f = \frac{1}{2}{p_{\hat{z}}}^2 + \frac{1}{2}\frac{1}{\hat{I}_f}{p_{\hat{\theta}}}^2 + \hat{g}_f\hat{z} + \frac{\hat{k}_f}{2}\left(\hat{z} - \hat{\theta}\right)^2.$$

In the front half cycle, the equations of motion become,

$$\begin{aligned}&\hat{\dot{\theta}} = \frac{\partial \hat{H}_f}{\partial p_{\hat{\theta}}},\quad \hat{\dot{z}} = \frac{\partial \hat{H}_f}{\partial p_{\hat{z}}},\quad \dot{p}_{\hat{\theta}} = -\frac{\partial \hat{H}_f}{\partial \hat{\theta}} = -\hat{k}_f\left(\hat{z} - \hat{\theta}\right),\\ &\dot{p}_{\hat{z}} = -\frac{\partial \hat{H}_f}{\partial \hat{z}} = -\hat{k}_f\left(\hat{z} - \hat{\theta}\right) - \hat{g}_f.\end{aligned} \tag{11}$$

For convenience, the "*hat*" notation is omitted in the remaining analysis, but all of the quantities presented are either rear or front normalized.

B. Poincaré Map

A Poincaré map is used for the stability analysis of bounding with each half cycle divided into phases: Top-to-Touchdown, Touchdown-to-Liftoff, and Liftoff-to-Top. The model falls freely from a maximum or "top" height in its flight phase with the initial conditions $(z_0, \dot{z}_0, \theta_0, \dot{\theta}_0)$, where $\dot{z}_0 = 0$ and $\dot{\theta}_0 < 0$. Without loss of generality, the rear leg is the first to contact and leave the ground before the body reaches a different maximum height, which then marks the start of the Top to Touchdown phase in the front half cycle. When the body reaches its maximum height at the end of the front half cycle, the state is $(z_6, \dot{z}_6, \theta_6, \dot{\theta}_6)$. The system has a periodic trajectory if the following equality constraints are satisfied:

$$\theta_6 = \theta_0, \text{ and } \dot{\theta}_6 = \dot{\theta}_0.$$

No condition on the vertical height of the mass center is necessary because it is not independent of these other two conditions.

The orbits of the Poincaré map corresponding to the fixed energy level Hamiltonian are periodic. Therefore, the stability is considered from cross section $\sum_0\{\dot{z}_0 = 0, \dot{\theta}_0 < 0\}$ to cross section $\sum_6\{\dot{z}_6 = 0, \dot{\theta}_6 < 0\}$ on the Poincaré map. With the original definitions of the conjugate momenta, each cross section is coordinated by $\left(\theta, p_\theta\right)$, independent of the rear and front normalizations. The Poincaré map is expressed as,

$$P : \textstyle\sum_0 \to \sum_6,$$

and is linearized as,

$$\begin{bmatrix}\delta p_{\theta 6}\\ \delta\theta_6\end{bmatrix} = A\begin{bmatrix}\delta p_{\theta 0}\\ \delta\theta_0\end{bmatrix}. \tag{12}$$

The eigenvalues of the 2×2 matrix A indicate the stability of a periodic solution.

C. Motion with Infinite Leg Stiffness

In order to further simplify the calculations, the leg stiffnesses k_f and k_r are assumed to approach infinity, so the time spent in the Touchdown-to-Liftoff phase approaches zero. A new variable $p = p_\theta + p_z$ is defined. The derivative of p with respect to time t is given by,

$$\dot{p} = \dot{p}_\theta + \dot{p}_z = -g_r,$$

so the rate change of p is finite. Since the time interval of ground contact is infinitesimal, p remains constant across the impact. Therefore,

$$p_{\theta 2} + p_{z2} = p_{\theta 1} + p_{z1}. \tag{13}$$

The impact between the leg and the ground is assumed to be a perfectly elastic collision, so the total energy of the system is conserved,

$$\frac{1}{I_r}p_{\theta 2}^2 + p_{z2}^2 = \frac{1}{I_r}p_{\theta 1}^2 + p_{z1}^2 = 2\left(H_r - g_r z\right) = 2\bar{H}_r. \tag{14}$$

After the impact, the angular position of the body and the height of the mass center remain the same as those before the impact. Therefore,

$$\theta_1 = \theta_2,\ z_1 = z_2. \tag{15}$$

Applying (15) to (13) and (14) yields,

$$\begin{aligned}p_{\theta 2} &= \frac{2I_r}{I_r+1}p_{z1} + \frac{I_r - 1}{I_r + 1}p_{\theta 1},\\ p_{z2} &= -\frac{I_r - 1}{I_r + 1}p_{z1} + \frac{2}{I_r+1}p_{\theta 1}.\end{aligned} \tag{16}$$

Through a similar procedure, the equations of motion in the front half cycle are obtained as,

$$\begin{aligned}p_{\theta 5} &= \frac{2I_f}{I_f+1}p_{z4} + \frac{I_f - 1}{I_f + 1}p_{\theta 4},\\ p_{z5} &= -\frac{I_f - 1}{I_f + 1}p_{z4} + \frac{2}{I_f+1}p_{\theta 4}.\end{aligned} \tag{17}$$

D. Hamiltonian Stability Analysis

1) Derivation of A_i

Linearization of the Poincaré map around the periodic trajectory yields a matrix A such that,

$$A : \left(\delta p_{\theta 0}, \delta\theta_0\right) \to \left(\delta p_{\theta 6}, \delta\theta_6\right).$$

The operator A is defined in (12) and is the product of matrices A_i, where $A_i : (\delta p_{\theta i-1}, \delta\theta_{i-1}) \to (\delta p_{\theta i}, \delta\theta_i)$ and $i = 1 \sim 6$.

The derivation of matrix A_2 is as follows. From (14) and (16),

$$p_{\theta 2} = -\frac{2I_r}{I_r+1}\sqrt{2\bar{H}_r - p_{\theta 1}^2/I_r} + \frac{I_r-1}{I_r+1}p_{\theta 1}. \qquad (18)$$

Differentiating (18) with respect to $p_{\theta 1}$ gives,

$$\frac{\partial p_{\theta 2}}{\partial p_{\theta 1}} = \frac{I_r}{I_r+1}\frac{2\,p_{\theta 1}/I_r}{\sqrt{2\bar{H}_r - p_{\theta 1}^2/I_r}} + \frac{I_r-1}{I_r+1}. \qquad (19)$$

Applying (14) to (19) yields,

$$\frac{\partial p_{\theta 2}}{\partial p_{\theta 1}} = -\frac{I_r}{I_r+1}\frac{2\,p_{\theta 1}/I_r}{p_{z1}} + \frac{I_r-1}{I_r+1}. \qquad (20)$$

Since the collision between the legs and the ground is perfectly elastic, it is assumed that,

$$p_{z2} = -p_{z1}, \quad p_{\theta 2} = -p_{\theta 1}. \qquad (21)$$

Note that in the most general case, (21) is not necessarily satisfied because the angular velocity and vertical velocity following the rear leg's impact could differ from those following the front leg's impact. Through these assumptions, the asymmetry of a bounding gait in this analysis is not related to the asymmetrical angular velocities in the two half cycles, but to the asymmetrical body structure. Simulation studies discussed in Section IV, however, indicate that this limitation does not significantly affect the validity of the derived stability criterion. From (13) and (21),

$$p_{\theta 1} = -p_{z1}. \qquad (22)$$

Therefore,

$$\frac{\partial p_{\theta 2}}{\partial p_{\theta 1}} = 1,$$

and,

$$\frac{\partial p_{\theta 2}}{\partial \theta_1} = \frac{\partial p_{\theta 2}}{\partial \bar{H}_r}\frac{\partial \bar{H}_r}{\partial \theta_1}. \qquad (23)$$

Differentiating (18) with respect to $\bar{H}_r$ yields,

$$\frac{\partial p_{\theta 2}}{\partial \bar{H}_r} = -\frac{I_r}{I_r+1}\frac{2}{\sqrt{2\bar{H}_r - p_{\theta 1}^2/I_r}} = -\frac{I_r}{I_r+1}\frac{2}{p_{\theta 1}}. \qquad (24)$$

When the rear leg contacts the ground, the normalized height of the rear leg z_r is equal to zero, which gives $z_1 + \theta_1 = 0$. Applying this condition to (14) gives,

$$\bar{H}_r = H_r - g_r z_1 = H_r + g_r\theta_1. \qquad (25)$$

Substituting (24) and (25) into (23) yields,

$$\frac{\partial p_{\theta 2}}{\partial \theta_1} = -\frac{2g_r I_r}{p_{\theta 1}\left(I_r+1\right)}. \qquad (26)$$

Thus,

$$\begin{bmatrix}\delta p_{\theta 2}\\ \delta\theta_2\end{bmatrix} = A_2\begin{bmatrix}\delta p_{\theta 1}\\ \delta\theta_1\end{bmatrix},$$

where,

$$A_2 = \begin{bmatrix}1 & W\\ 0 & 1\end{bmatrix},\; W = -\frac{2g_r I_r}{p_{\theta 1}\left(I_r+1\right)}.$$

Matrices A_1 and A_3 for the rear half cycle are derived in a similar fashion.

$$A_1 = \begin{bmatrix}1 & 0\\ R & L\end{bmatrix},\; A_3 = \begin{bmatrix}1 & 0\\ R/L & 1/L\end{bmatrix},$$

where,

$$R = -\frac{I_r-1}{I_r+1}\frac{\dot{\theta}_0}{g_r},\; L = \frac{I_r}{I_r+1}.$$

In the front half cycle, the matrices A_4, A_5, and A_6 are,

$$A_4 = \begin{bmatrix}1 & 0\\ B & J\end{bmatrix},\; A_5 = \begin{bmatrix}1 & M\\ 0 & 1\end{bmatrix},\; A_6 = \begin{bmatrix}1 & 0\\ B/J & 1/J\end{bmatrix},$$

where,

$$M = \frac{2g_f I_f}{p_{\theta 4}\left(I_f+1\right)},\; B = \frac{I_f-1}{I_f+1}\frac{\dot{\theta}_3}{g_f},\; J = \frac{I_f}{I_f+1}.$$

2) Stability Analysis

The linearized return maps for the rear and front half cycles are given by,

$$\begin{bmatrix}\delta p_{\theta 3}\\ \delta\theta_3\end{bmatrix}_r = A_3 A_2 A_1\begin{bmatrix}\delta p_{\theta 0}\\ \delta\theta_0\end{bmatrix}_r, \qquad (27)$$

and,

$$\begin{bmatrix}\delta p_{\theta 6}\\ \delta\theta_6\end{bmatrix}_f = A_6 A_5 A_4\begin{bmatrix}\delta p_{\theta 3}\\ \delta\theta_3\end{bmatrix}_f. \qquad (28)$$

In order to combine (27) and (28) to investigate the properties of an entire stride cycle, a transformation between rear-normalized and front-normalized quantities is necessary. Noting the difference between the normalizations, the transformation can be simply expressed as,

$$\left[\delta p_\theta\right]_f = I_f/I_r\left[\delta p_\theta\right]_r,\quad \left[\delta\theta\right]_f = \left[\delta\theta\right]_r. \qquad (29)$$

Applying (29) to (27) and (28) gives,

$$\begin{bmatrix}\delta p_{\theta 6}\\ \delta\theta_6\end{bmatrix}_f = A\begin{bmatrix}\delta p_{\theta 0}\\ \delta\theta_0\end{bmatrix}_f,$$

where the diagonal entries of A are,

$$A_{11} = \left(1+MB\right)\left(1+WR\right) + \frac{I_r}{I_f}\frac{J}{L}MR\left(2+WR\right),$$

$$A_{22} = \left(1+MB\right)\left(1+WR\right) + \frac{I_f}{I_r}\frac{L}{J}MB\left(2+MB\right).$$

The characteristic equation of the matrix A is,

$$\lambda^2 - tr\left(A\right)\lambda + det\left(A\right) = 0,$$

where $tr\left(A\right)$ is the trace of A and $det\left(A\right)$ is its determinant. The eigenvalues of A are given by,

$$\lambda = \frac{1}{2}\left(tr\left(A\right) \pm \sqrt{tr\left(A\right)^2 - 4\,det\left(A\right)}\right).$$

Since the determinant of matrix A is 1, the system is stable if $\left|tr\left(A\right)\right| < 2$. The stability condition becomes,

$$-2 < A_{11} + A_{22} < 2. \qquad (30)$$

E. Stability Criterion for Bounding

A new variable β is defined as $\beta = d/l$, where $0 < \beta < 1$. The dimensionless moments of inertia defined in (3) and (8) can be expressed in terms of β as,

$$I_r = \frac{I_0}{(1+\beta)^2}, \quad I_f = \frac{I_0}{(1-\beta)^2}. \tag{31}$$

where $I_0 = I/ml^2 > 0$.

The right hand side of (30) is,

$$A_{11} + A_{22} - 2 < 0. \tag{32}$$

Substituting and factoring (32) yields,

$$\frac{I_0\left(I_0 - 1 + \beta^2\right)\left(3\beta^4 + 3I_0\beta^2 - 6\beta^2 + 3 + I_0\right)}{\left(\beta^2 - 1\right)\left(I_0 + \beta^2 + 1 - 2\beta\right)^2\left(I_0 + \beta^2 + 1 + 2\beta\right)^2} > 0. \tag{33}$$

The first term in the denominator is negative, so it can be concluded that (33) is satisfied if $I_0 - 1 + \beta^2 < 0$ since,

$$3\beta^4 + 3I_0\beta^2 - 6\beta^2 + 3 + I_0 = I_0(3\beta^2 + 1) + 3(\beta^2 - 1)^2 > 0.$$

Therefore,

$$I_0 < 1 - \beta^2.$$

The left hand side of (30) is rewritten as,

$$A_{11} + A_{22} + 2 > 0. \tag{34}$$

Substituting and factoring (34) gives,

$$\frac{(U - V)(U + V)}{\left(\beta^2 - 1\right)\left(I_0 + \beta^2 + 1 - 2\beta\right)^2\left(I_0 + \beta^2 + 1 + 2\beta\right)^2} > 0, \tag{35}$$

where,

$$U = \beta I_0^2 - 6I_0\beta + \beta + 2I_0\beta^3 - 2\beta^3 + \beta^5,$$

$$V = I_0^2 + 4I_0 - 1 + 2\beta^2 + \beta^4.$$

The denominator in (35) is identical to that in (33), so it is again negative. For brevity, the details are not presented here, but by calculating the extreme values of the numerator in (35) and examining its values along the boundaries for the acceptable ranges of I_0 and β, it can be shown that,

$$(U - V)(U + V) = U^2 - V^2 < 0.$$

Therefore, (35) is satisfied, as is the left hand side of (30), regardless of the values β and I_0 take on in their prescribed intervals.

Hence, the bounding motion is passively stable for a quadruped with an asymmetrical body provided that,

$$I_0 < 1 - \beta^2. \tag{36}$$

Neishtadt and Li's [12] and Berkemeier's [1] stability criterion for a symmetrical body, simply that I_0 is less than unity, is embedded within (36) because $\beta = 0$ in the symmetric case. Since the range of dimensionless inertia values for which passively stable bounding can be achieved with a symmetrical body is larger than that for an asymmetrical body, it can be concluded that the asymmetry is at least somewhat detrimental to stability. In a practical sense, however, the value of β is typically small - about 0.2 for most biological quadrupeds [2] [3] [5] [10]. Therefore, unless the asymmetry is extreme, the critical value of dimensionless inertia is nearly the same as in the symmetrical case. With a well designed system characterized by dimensionless inertia far from the critical value anyway, asymmetry in body mass distribution does not pose significant problems for generating stable bounding gaits.

IV. Simulation Results

A number of simulations were performed to examine the validity of the stability criterion (36) for finite values of leg stiffness and for non-zero leg damping and thrust. All simulations were executed in Simulink using fixed-step Dormand-Prince integration. For the results presented here, k is 30 *kN/m*, m is 30 kg, l is 0.35 m, and d is 0.06 m, so by application of (36), the critical value of the dimensionless moment of inertia is 0.971. Figs. 2, 3, and 4 each plot 30 full bounding cycles.

In Fig. 2, the bounding gait is stable when I_0 has a value of 0.967 (less than the critical value), and the asymmetry of the gait is clearly seen by the two different values for the height of the mass center when the front and rear legs are maximally compressed (i.e. the two different local minima in the orbit). In Fig. 3, the bounding gait is unstable when I_0 has a value of 0.975 (greater than the critical value). These two plots, and additional simulation results not presented here, indicate that in the absence of energy loss, the stability criterion (36) is valid regardless of the value of leg stiffness in the model. The criterion was derived with the assumption of infinite leg stiffness, but simulation results for very small stiffness values show no dependence of the critical inertia value on leg

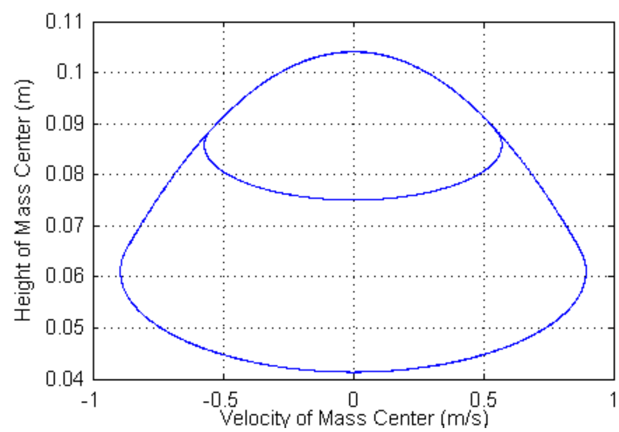

Figure 2. Simulation of bounding as $I_0 = 0.967$ without energy loss.

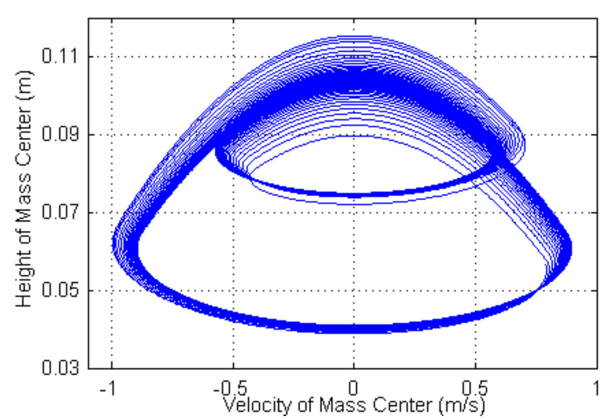

Figure 3. Simulation of bounding as $I_0 = 0.975$ without energy loss.

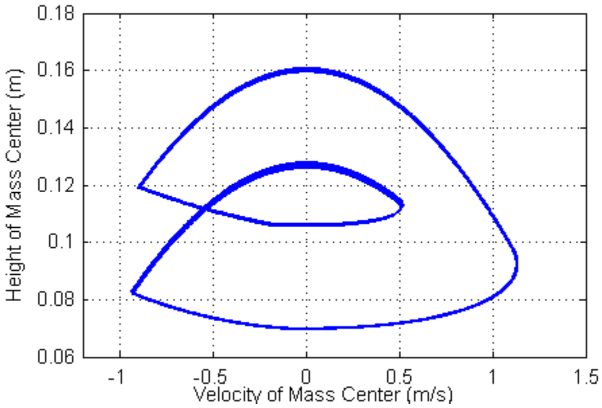

Figure 4. Simulation of bounding as $I_0 = 0.980$ with energy loss.

stiffness. These results are in direct contrast with Neishtadt and Li's [12] conclusion that the critical value decreases as leg stiffness decreases. Because no simulation results comparable to those in this work were presented, the discrepancy might be explained by modeling assumptions made in deriving the analytical stability criterion as a function of leg stiffness.

The critical value of inertia is dependent, however, upon parameter changes in leg damping and thrust when they become non-zero to model energy losses and corresponding energy input to the system. No similar result has been presented in previous work addressing symmetrical models. Fortunately, the critical value of I_0 becomes increasingly larger than the predicted value of (36) as damping and thrust increase. Fig. 4 is an example of stable bounding when I_0 is 0.980 (greater than the predicted critical value) and the damping coefficient b is non-zero. These results suggest that (36) is actually a conservative estimate of the critical value for dimensionless body inertia. Additional simulation results indicate that for even very large damping coefficients, the critical value is not significantly larger than the predicted value. Therefore, (36) can be applied directly as a design criterion for quadrupeds capable of bounding.

V. CONCLUSIONS

The stability of a planar quadruped model with asymmetrical mass distribution was analyzed to derive a new, analytical criterion for passively stable bounding. The criterion states that bounding is passively stable provided a dimensionless moment of inertia is less than $1-\beta^2$, where β is a dimensionless measure of the asymmetry. This result is in agreement with previously derived criteria for symmetrical quadruped models [1] [12]. Symmetry appears to be more favorable to stable bounding, but only slightly so in practicality. In contrast to a previous study [12], simulation results in this work suggest that the derived criterion is applicable regardless of the value of leg stiffness in the model. When energy losses are modeled with linear damping, however, the stability condition is still reasonably valid, although simulation results suggest that the critical value of inertia increases slightly as damping increases.

The authors hope that this work will enable robot designers to consider the merits of body asymmetry in developing quadrupeds capable of efficient, dynamically stable locomotion. The results indicate that the asymmetrical body mass distribution common in biological quadrupeds, but rare in robotic quadrupeds does not have a significantly adverse effect on pitch stability in bounding.

REFERENCES

[1] M. D. Berkemeier, "Modeling the dynamics of quadrupedal running," International Journal of Robotics Research, vol. 17, no. 9, pp. 971-985, 1998.

[2] C. M. Brown, Dog Locomotion and Gait Analysis. Hoflin Publishing, Wheat Ridge, Colorado, 1986.

[3] J. D. Bryant, M. B. Bennett, J. Brust, and R. McN. Alexander, "Forces exerted on the ground by galloping dogs," Journal of Zoology, London, vol. 213, pp. 193-203, 1987.

[4] J. Furusho, S. Akihito, S. Masamichi, and K. Eichi, "Realization of bounce gait in a quadruped robot with articular-joint-type-legs," Proceedings of the IEEE International Conference on Robotics and Automation, Piscataway, New Jersey, pp. 697-702, 1995.

[5] A. S. Jayes, and R. M. Alexander, "Mechanics of locomotion in dogs and sheep," Journal of Zoology, London, vol. 185, pp. 289-308, 1978.

[6] H. Kimura, S. Akiyama, and K Sakurama, "Realization of Dynamic Walking and Running of the Quadruped Using Neural Oscillator," Autonomous Robots, vol. 7, no. 3, pp. 247-258, 1999.

[7] H. Kimura, Y. Fukuoka, Y. Hada, and K. Takase, "Three-dimensional Adaptive Dynamic Walking of a Quadruped – rolling motion feedback to CPG's controlling pitching motion," Proceedings of the IEEE International Conference on Robotics and Automation, Washington D.C., pp. 2228-2233, 2002.

[8] D. E. Koditschek, and M. Bühler, "Anlysis of a Simplified Hopping Robot," International Journal of Robotics Research, vol. 10, no. 6, pp. 587-605, 1991.

[9] Z. Li, and J. He, "An Energy Perturbation Approach to Limit Cycle Analysis in Legged Locomotion Systems," Proceedings of the 29th Conference on Decision and Control, Honolulu, Hawaii, pp. 1989-1994, 1990.

[10] J. T. Manter, "The dynamics of quadrupedal walking," Jounral of Experimental Biology, vol. 15, pp. 522-540, 1938.

[11] R. T. M'Closkey, and J. W. Burdick, "Periodic Motions of a Hopping Robot with Vertical and Forward Motion," International Journal of Robotics Research, vol. 12, no. 3, pp. 197-218, 1993.

[12] A. Neishtadt, and Z. Li, "Stability proof of Raibert's four-legged hopper in bounding gait," Technical Report No. 578, New York University, 1991.

[13] D. Papadopoulos and M. Bühler, "Stable Running in a Quadruped Robot with Compliant Legs," Proceedings of the IEEE International Conference on Robotics and Automation, San Francisco, California, pp. 444-449, 2000.

[14] M. H. Raibert, Legged Robots that balance, MIT Press, Cambridge, MA, 1986.

[15] M. H. Raibert, "Trotting, pacing and bounding by a quadruped robot," Journal of Biomechanics. vol. 23, suppl. 1, pp. 79-98, 1990.

[16] M. H. Raibert, H. B. Brown, M. Chepponis, J. Hodgins, J. Koechling, J. Miller, K. N. Murphy, S. S. Murthy, and A. Stentz, "Dynamically stable legged locomotion," Technical Report CMU-LL-4-1985, Carnegie-Mellon University, Pittsburgh, 1985.

[17] J. P. Schmiedeler and K. J. Waldron, "The mechanics of quadrupedal galloping and the future of legged vehicles," International Journal of Robotics Research, vol. 18, no. 12, pp. 1224-1234, 1999.

[18] A. F. Vakakis, J. W. Burdick, and T. K. Coughey, "An 'Interesting' Strange Attractor in the Dynamics of a Hopping Robot," International Journal of Robotics Research, vol. 10, no. 6, pp. 606-618, 1991.